Hindawi
Mathematical Problems in Engineering
Volume 2019, Article ID 1345364, 14 pages
https://doi.org/10.1155/2019/1345364

Research Article

Parameter Identification of Tractor-Semitrailer Model under Steering and Braking

Yiming Li, Qin Shi, and Duoyang Qiu

School of Automobile and Transportation Engineering, Hefei University of Technology, No. 193 Tunxi Road, Hefei, Anhui 230009, China

Correspondence should be addressed to Yiming Li; lymzhijia@163.com

Received 24 May 2019; Revised 12 August 2019; Accepted 21 August 2019; Published 10 September 2019

Academic Editor: Ning Sun

This paper describes a valuable linear yaw-roll tractor-semitrailer (TST) model with five-degree-of-freedom (DOFs) for control algorithm development when steering and braking. The key parameters, roll stiffness, axle cornering stiffness, and fifth-wheel stiffness, are identified by the genetic algorithm (GA) and multistage genetic algorithm (MGA) based on TruckSim outputs to increase the accuracy of the model. Thus, the key parameters of the simplified model can be modified according to the real-time vehicle states by online lookup table and interpolation. The TruckSim vehicle model is built referring to the real tractor (JAC-HFC4251P1K7E33ZTF6×2) and semitrailer (Luyue LHX9406) used in the field test later. The validation of the linear yaw-roll model of a tractor-semitrailer using field test data is presented in this paper. The field test in the performance testing ground is detailed, and the test data of roll angle, roll rate, and yaw rate are compared with the outputs of the model with maps of the key parameters. The results indicate that the error of the tractor's roll angle and semitrailer's roll angle between model data and test data is 1.13% and 1.24%, respectively. The roll rate and yaw rate of the tractor and semitrailer are also in good agreement.

1. Introduction

Tractor-semitrailers (TSTs) are commonly used in road freight transportation all over the world. The popularity of such vehicles is due to their flexibility and transport efficiency. The most popular vehicles of this type consist of a tractor unit or prime mover coupled to a long semitrailer [1]. Because of the complex structure, large size, and high center of gravity, the low-speed maneuverability and high-speed lateral stability of TST systems are limited [2]. An effective solution to this issue is the application of active steering [3]. Although active trailer steering (ATS) was proved to be effective, a further improvement in low-speed maneuverability and high-speed lateral stability can be obtained using more advanced dynamic models.

The linear simple model is widely used in designing control algorithms and strategies. It offers considerably shorter simulation run time and is simpler and faster to change any parameters [4]. But the linear model is only suitable for a small range of slip angle and lateral acceleration (below 0.4 of gravitational acceleration) on account of assumptions made in its derivation [5]. The control performances are limited in high-speed cases [6,7]. In Wang's research, a linear yaw-roll model was developed to design the linear quadratic ATS controller of the tractor-two-semitrailer system [6]. The controller was simulated in the high-speed manoeuvres of 88 km/h and 120 km/h. The amplitude of the lateral acceleration was limited to 0.15 g. Compared with the case without ATS, the controller evidently reduced the yaw rate of two semitrailers. But the lateral acceleration of the first semitrailer was even higher under ATS control. And the second articulation angle was 80% higher under ATS control. Similarly, Ding generated a 4-DOF linear yaw-plane model of the tractor-two-semitrailer system [7]. The linear quadratic regulator (LQR), based on the linear model, was applied to the ATS controller design. Then, the controller was simulated in the cases of a low-speed 90-degree intersection turn, a low-speed 360-degree roundabout path-following manoeuvre, and a high-speed single-lane-change manoeuvre. In the low-speed cases, the path-following off-tracking and rearward

amplification ratio were, respectively, decreased up to 87.5% and 40.7%. But in the high-speed single-lane-change manoeuvre, the rearward amplification ratio was only decreased by 29.5% because the nonlinear characteristic in the high-speed case is higher than that in the low-speed case. When the slip angle and lateral acceleration overstep the limit range, the nonlinear characteristics of the vehicle are intensified. In this condition, the model cannot be simplified into a linear model.

In order to generate more accurately the nonlinear TST model, the nonlinear tyre models (presented by Pacejka) are used in Kharrazi and Oreh's researches. Controllers are designed based on the nonlinear vehicle models. A steering-based simple controller is presented in Kharrazi's research [8]. The controller effectiveness analysis in frequency and time domains demonstrates that the yaw rate rearward amplification and off-tracking were significantly reduced by the steering-based controller. But the control improvement of the first trailer was not obvious to the last trailers, and even not comparable to the other control models. Oreh presents a linear quadratic regulator (LQR) controller, a nonlinear sliding-mode controller (SMC) [9], and a fuzzy-supervised proportion-integration-differentiation (PID) controller [10] based on the same 12-DOF nonlinear TST model with the magic formula model (presented by Pacejka). The SMC was compared with the LQR controller to verify the veracity of the nonlinear model. The controllers were simulated with different adhesion coefficients and a single sinusoidal steering angle. The simulation results show that the performance of the SMC was better than that of the linear controller in many manoeuvres. However, for the LQR controller, the sideslip angle was smaller than that of the SMC controller. The controlling effect of the new fuzzy-supervised PID controller was almost the same with the SMC he designed before. Above all, there are deficiencies in the control results in Kharrazi and Oreh's researches. Because the two problems listed below are ignored in their nonlinear vehicle models.

Firstly, the lateral force obtained by the nonlinear tyre model is not accurate enough. The sideslip angles of each tyre are essential input variables of the nonlinear tyre model. On account of the flexibility of suspension and a different center location of each tyre, the sideslip angles of each tyre are different. The lateral force increase at the outside tyre is usually smaller than the lateral force decrease at the inside tyre because of the nonlinearity of the tyre and suspension [11]. In addition, there are always two tyres on the same side in one axle of the semitrailer. The nonlinear characteristics of the inner and outside tyres are different. The tyre cornering stiffness cannot be superposed linearly based on the single nonlinear tyre model.

Secondly, the nonlinear characteristics of the real vehicle listed below are not exhaustively considered in their models. In a real TST, there are uncertainties in the vehicle dynamics such as the inertia parameters, the friction coefficient, and the tyre's cornering stiffness [9]. Actually, the suspension also exhibits nonlinearity between components. Overall, the roll stiffness of the vehicle suspension is not constant as presented in the nonlinear models above.

The nonlinear characteristics of all the components have to be determined by the field test with advanced sensors and are very costly. Therefore, identification of these nonlinear characteristics would be a logical choice [12]. Nie and Zong, Kim et al., and Guang et al. mentioned that it is not necessary to model all the nonlinear components rather than generally characterize their overall nonlinear property related to the vehicle's dynamics [13–16]. But in Nie and Zong, Kim et al., and Guang et al.'s researches, there are two main inadequacies.

Primarily, in Nie and Zong, Kim et al., and Guang et al.'s researches, the stationary turning condition and step steering condition are considered to identify parameters. The design variables of parameter identification are longitudinal speed, steering wheel angle, and lateral acceleration. According to their results, in steering and braking conditions, the key parameters of the TST model are identified as the same as those under the same longitudinal speed but different deceleration. According to Newton's first law of motion, every object in a state of uniform motion tends to remain in that state of motion unless an unbalanced force is applied to it. When the TST was under a steering and braking condition, both the lateral acceleration and the longitudinal deceleration were affected by the lateral force. Actually, when the TST is braking at the same speed (larger than zero), the force, the roll angle of the sprung mass, and the sideslip angle of the tyre were all affected by the deceleration. During braking, the instantaneous velocities are changed over time. It is hard to identify the stiffness at every moment. Hence, we identified the key parameters of the vehicle model under steering and braking conditions. The deceleration and steering wheel angle were set as constant under each condition.

In the second place, the roll stiffness of the fifth wheel was set as constant in their researches. Actually, the complicated structure and the placement of the fifth wheel result in the nonlinear characteristics [4]. In our experiment, the roll angles of the tractor and semitrailer made a big difference. The fifth-wheel stiffness had a great impact on the dynamics of the tractor and semitrailer. Therefore, the fifth-wheel stiffness was also considered one of the key parameters identified in this paper. In this paper, the fifth-wheel stiffness, roll stiffness, and cornering stiffness are identified at the specified deceleration and steering wheel angle.

Above all, the condition and object variables of identification were confirmed. Then, the identification problem is solved as an optimization problem, and the search technique is a critical factor in determining the performance of the optimization scheme. Many search techniques are used in identifying characteristics of the TST model, for example, the trial-and-error method [11], least-square method [17], particle swarm optimization [15, 16], and genetic algorithm [13, 14]. In this paper, a large number of possible solutions to the parameters of the linear TST model suggest that the GA is effective and accurate [18, 19]. The genetic algorithm is a mature method for optimization. It works well under a few objectives. In this research, there are 6 objectives (cornering stiffness of the tractor's front axle, cornering stiffness of the tractor's rear axle, cornering stiffness of the semitrailer's

axle, roll stiffness of the tractor's sprung mass, roll stiffness of the semitrailer's sprung mass, and roll stiffness of the fifth wheel). The traditional GA is prone to fall into local optimal solutions under 6 objectives. In consequence, we propose a new multistage genetic algorithm (MGA) to improve the precision of identification and avoid the local optimal solution problems.

This paper is organized as follows: Section 2 builds the linear TST model based on the one-dimensional bicycle model with two bodies and 5 DOFs. Section 3 introduces the identification algorithm based on the GA and MGA and then generates the parameter maps by the linear interpolation method. Section 4 presents the field test of the TST during steering and braking. Section 5 verifies the accuracy of the linear model with parameter maps by contrasting the output of the model and the real vehicle testing. Section 6 presents a conclusion.

2. Linear 5-DOF Tractor-Semitrailer Model

In this section, a linear TST model, namely, 5-degree-of-freedom (5-DOF) model, is derived. To ensure that the linear model can reflect the model more accurately, the parameters of the linear model are obtained from the JAC-HFC4251P1K7E33ZTF6×2 tractor and Luyue LHX9406 semitrailer, as shown in Table 1. The two rear axles of the tractor and the axles of the semitrailer all have two tyres (CHAOYANG MD738-12R22.5-152/149L) on one side. The semitrailer was of hurdle-plate type, as shown in Figure 1; the 5-DOF model includes the dynamics of the lateral, yaw, and roll velocities of the sprung masses (the tractor and semitrailer).

To develop a linear TST model, the sideslip stiffness of the tyre, the roll stiffness, and the fifth-wheel stiffness are assumed to be constant. The aerodynamics, road grade, load transfer, and transmission system of the steering system are neglected to simplify the model [20]. The pitching motions of the tractor and semitrailer are small because of the fifth wheel. The comfort is also not researched in this paper. Therefore, the pitch and bounce are neglected [10]. The steering wheel angle and longitudinal speed are used directly as the system input. The longitudinal speed is time varying in the simulation; therefore, the longitudinal deceleration is considered the first-order derivative of the longitudinal speed. The longitudinal deceleration is assumed to be consistent during brake to simplify the identification conditions. In this paper, the linear TST model is associated with the offline parameter map, so the key parameters (roll stiffness, axle cornering stiffness, and fifth-wheel stiffness) are assumed as constant.

The assumptions of the TST model are listed as follows:

(1) The aerodynamics and road grade are neglected

(2) The load transfer is neglected

(3) The transmission system of the steering system is ignored, and the steering wheel angle is used directly as the system input

(4) The longitudinal acceleration is considered the first-order derivative of the longitudinal speed, and the varying longitudinal speed is used directly as the system input

(5) The tractor and the semitrailer units have no pitch or bounce

(6) The articulation angle of the fifth wheel is small [15]

(7) The relationship between the tyre force and the sideslip angle is linear

(8) The relationship between the roll moment and the roll angle is linear

(9) The roll moment transmitted by the fifth wheel is assumed to be proportional to the relative roll angle and relative roll rate between the two units [21]

The equations of vehicle motions of the tractor unit are built based on Newton's second law of motion (see nomenclature) [20]:

$$\begin{aligned} m_t v_{tx}\left(\dot{\varphi}_t + \dot{\beta}_t\right) - m_t h_t \ddot{\theta}_t &= F_1 + F_2 + F_3, \\ I_{tzz}\ddot{\varphi}_t &= F_1 l_1 - F_2 l_2 - F_3 l_3, \\ I_{txx}\ddot{\theta}_t + \ddot{\theta}_t h_t^2 M_{ts} - v_{tx} M_t h_t\left(\dot{\varphi}_t + \dot{\beta}_t\right) &= m_t g h_t \theta_t - K_{rt}\theta_t - C_{rt}\dot{\theta}_t \\ &\quad - K_F\left(\theta_t - \theta_s\right) - F_3 h_{tF}. \end{aligned} \tag{1}$$

The equations of semitrailer motions are

$$\begin{aligned} m_s v_{sx}\left(\dot{\varphi}_s + \dot{\beta}_s\right) - m_s h_s \ddot{\theta}_s &= F_4 - F_3\cos\gamma, \\ I_{szz}\ddot{\varphi}_s &= -F_4 l_5 - F_3 l_4 \cos\gamma, \\ I_{sxx}\ddot{\theta}_s + \ddot{\theta}_s h_s^2 M_{ss} - v_{sx} M_s h_s\left(\dot{\varphi}_s + \dot{\beta}_s\right) &= m_s g h_s \theta_s - K_{rs}\theta_s \\ &\quad - C_{rs}\dot{\theta}_s + K_F\left(\theta_t - \theta_s\right) \\ &\quad + F_3 h_{sF}\cos\gamma. \end{aligned} \tag{2}$$

The kinematic constraint equation of the fifth wheel is

$$-\left(\dot{\varphi}_t + \dot{\beta}_t\right) l_3 - \dot{\theta}_t h_{tF} = \left(\dot{\varphi}_s + \dot{\beta}_s\right) l_4 - \dot{\theta}_s h_{sF}. \tag{3}$$

The tyre side forces acting on the articulated vehicle are generated at the contact patch between the tyre and the road. Note that, in generating the 5-DOF model, the tyre properties are linearized, and the effects of the camber thrust, the roll steer, and the aligning moment are neglected. The tyre side forces are [22]

$$\begin{aligned} F_1 &= K_1\left(\beta_t + \frac{l_1\dot{\varphi}_t}{v_{tx}} - \alpha\right), \\ F_2 &= K_2\left(\beta_t - \frac{l_3\dot{\varphi}_t}{v_{tx}}\right), \\ F_3 &= K_3\left(\beta_s - \frac{l_5\dot{\varphi}_s}{v_{sx}}\right). \end{aligned} \tag{4}$$

Table 1: Nomenclature.

Parameter	Symbol	Unit
Fifth-wheel stiffness	K_F	N·m/rad
Roll stiffness of the tractor	K_{rt}	N·m/rad
Roll stiffness of the semitrailer	K_{rs}	N·m/rad
Cornering stiffness of the tractor's front axle	K_1	N/rad
Cornering stiffness of the tractor's rear axle	K_2	N/rad
Cornering stiffness of the semitrailer's axle	K_3	N/rad
Tractor's speed	v_{tx}	m/s
Semitrailer's speed	v_{sx}	m/s
Tractor's sideslip angle	β_t	Rad
Semitrailer's sideslip angle	β_s	Rad
Tractor's yaw rate	$\dot{\varphi}_t$	Rad/s
Semitrailer's yaw rate	$\dot{\varphi}_s$	Rad/s
Articulated angle	γ	Rad
Tractor's roll angle	θ_t	Rad
Semitrailer's roll angle	θ_s	Rad
Tractor's roll rate	$\dot{\theta}_t$	Rad/s
Semitrailer's roll rate	$\dot{\theta}_s$	Rad/s
Tractor's entire vehicle mass	m_t	kg
Semitrailer's entire vehicle mass	m_s	kg
Tractor's sprung mass	M_t	kg
Semitrailer's sprung mass	M_s	kg
Roll moment of inertia of the tractor's sprung mass	I_{txx}	kg·m^2
Roll moment of inertia of the semitrailer's sprung mass	I_{sxx}	kg·m^2
Yaw moment of inertia of the tractor's sprung mass	I_{tzz}	kg·m^2
Yaw moment of inertia of the semitrailer's sprung mass	I_{szz}	kg·m^2
Distance between the tractor CG and the front axle	l_1	m
Distance between the tractor CG and the rear axle	l_2	m
Distance between the tractor CG and the fifth wheel	l_3	m
Distance between the semitrailer CG and the axle	l_4	m
Distance between the semitrailer CG and the fifth wheel	l_5	m
Distance between the tractor CG and the roll axle line	h_t	m
Distance between the semitrailer CG and the roll axle line	h_s	m
Distance between the fifth wheel and the tractor roll axle line	h_{tF}	m
Distance between the fifth wheel and the semitrailer roll axle line	h_{sF}	m
Roll damping of the tractor's suspension	C_{rt}	N·s/m
Roll damping of the semitrailer's suspension	C_{rs}	N·s/m

The 5-DOF model can be expressed in the state-space form as follows:

$$\dot{\mathbf{X}} = \mathbf{A}\mathbf{X} + \mathbf{B}\alpha, \tag{5}$$

where

$$\mathbf{X} = \begin{bmatrix} \beta_t & \dot{\varphi}_t & \dot{\theta}_t & \theta_t & \beta_s & \dot{\varphi}_s & \dot{\theta}_s & \theta_s \end{bmatrix}^T,$$
$$\mathbf{A} = \mathbf{M}^{-1}\begin{bmatrix} \mathbf{A}_{11} & \cdots & \mathbf{A}_{18} \\ \vdots & \ddots & \vdots \\ \mathbf{A}_{81} & \cdots & \mathbf{A}_{88} \end{bmatrix},$$
$$\mathbf{B} = \mathbf{M}^{-1}\begin{bmatrix} -(l_1 + l_3)K_1 & -K_1 h_{tF} & 0 & 0 & 0 & -K_1 & 0 & 0 \end{bmatrix}^T,$$
$$\mathbf{M} = \begin{bmatrix} \mathbf{M}_{11} & \cdots & \mathbf{M}_{18} \\ \vdots & \ddots & \vdots \\ \mathbf{M}_{81} & \cdots & \mathbf{M}_{88} \end{bmatrix}. \tag{6}$$

X is the state variable vector. **A**, **B**, and **M** are the system matrix, the disturbance matrix, and the mass matrix.

The nonzero elements of **M** and **A** are presented in Appendix.

3. Stiffness Identification for the Tractor-Semitrailer Model

To reflect the main characteristic of the actual vehicle state by the simplified vehicle model, the key parameters are identified offline by the GA according to TruckSim data. Steering and braking conditions are adopted to identify the key parameters. The required key parameters include roll stiffness, axle cornering stiffness, and fifth-wheel stiffness.

To reflect the main characteristic of the actual vehicle state by the simplified vehicle model, the key parameters are identified offline by the GA and multistage GA according to TruckSim data. Steering and braking conditions are adopted to identify the key parameters. The required key parameters include roll stiffness, axle cornering stiffness, and fifth-wheel stiffness.

3.1. Stiffness Identification Based on GA. The genetic algorithm program used in this paper is compiled by the genetic algorithm toolbox in the software MATLAB. The flow diagram of the GA program is shown in Figure 2. To identify the parameters by the GA, it is necessary to define four components: (1) a fitness function to measure and compare different candidates; (2) random generation of an initial population of individuals; (3) selection of the individuals that are to be used for evolution; and (4) the survival criteria (crossover and mutation) to be accomplished for individuals that are conserved into the next generation, on each iteration. These components are described in the following.

3.1.1. Fitness Function. The fitness function is defined as the absolute value of error between the outputs of the simplified 5-DOF tractor-semitrailer model and TruckSim. The optimal values of each parameter are defined as the values which made the fitness function close to zero. The fitness function is defined by [13]

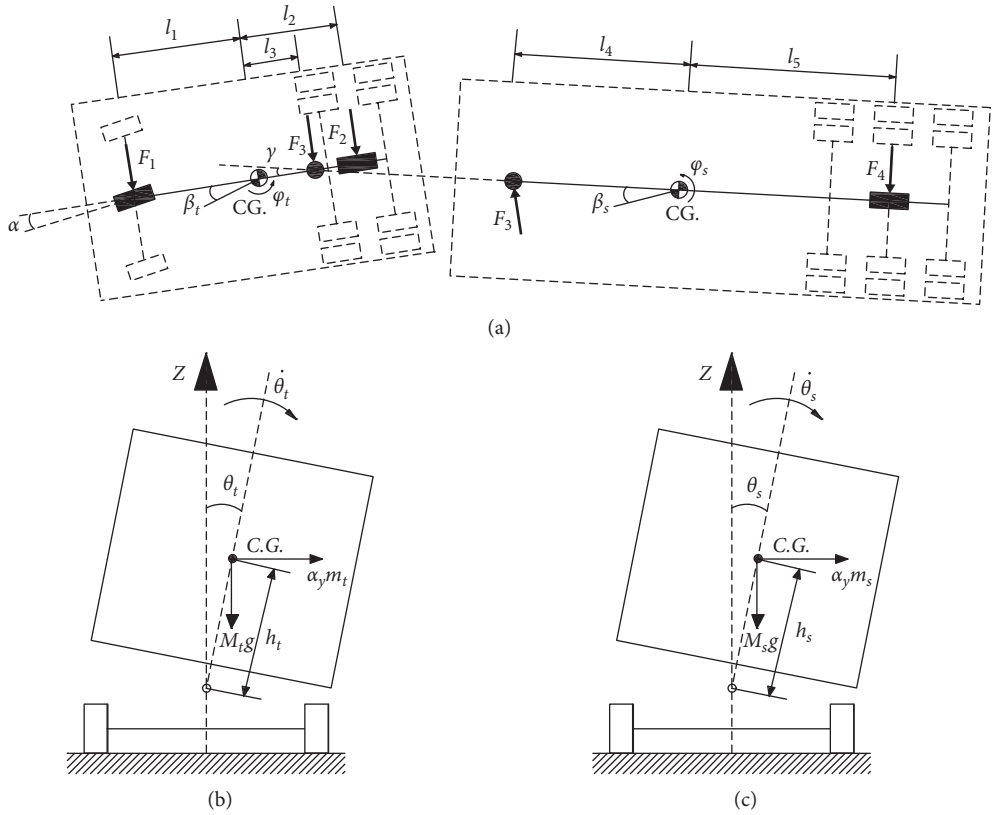

Figure 1: 5-DOF TST model: (a) yaw moment; (b) roll moment of the tractor; (c) roll moment of the semitrailer.

$$
\begin{aligned}
f = & \sum_{i=1}^{b}\left|\frac{\beta_{t-\text{model}}(i)-\beta_{t-\text{trucksim}}(i)}{\beta_{t-\text{trucksim}}(i)}\right| \\
& + \sum_{i=1}^{b}\left|\frac{\beta_{s-\text{model}}(i)-\beta_{s-\text{trucksim}}(i)}{\beta_{t-\text{trucksim}}(i)}\right| \\
& + \sum_{i=1}^{b}\left|\frac{\dot{\varphi}_{t-\text{model}}(i)-\dot{\varphi}_{t-\text{trucksim}}(i)}{\dot{\varphi}_{t-\text{trucksim}}(i)}\right| \\
& + \sum_{i=1}^{b}\left|\frac{\dot{\varphi}_{s-\text{model}}(i)-\dot{\varphi}_{s-\text{trucksim}}(i)}{\dot{\varphi}_{s-\text{trucksim}}(i)}\right| \\
& + \sum_{i=1}^{b}\left|\frac{\dot{\theta}_{t-\text{model}}(i)-\dot{\theta}_{t-\text{trucksim}}(i)}{\dot{\theta}_{t-\text{trucksim}}(i)}\right| \\
& + \sum_{i=1}^{b}\left|\frac{\dot{\theta}_{s-\text{model}}(i)-\dot{\theta}_{s-\text{trucksim}}(i)}{\dot{\theta}_{s-\text{trucksim}}(i)}\right| \\
& + \sum_{i=1}^{b}\left|\frac{\theta_{t-\text{model}}(i)-\theta_{t-\text{trucksim}}(i)}{\theta_{t-\text{trucksim}}(i)}\right| \\
& + \sum_{i=1}^{b}\left|\frac{\theta_{s-\text{model}}(i)-\theta_{s-\text{trucksim}}(i)}{\theta_{s-\text{trucksim}}(i)}\right|.
\end{aligned} \tag{7}
$$

The nomenclature is shown in Table 2.

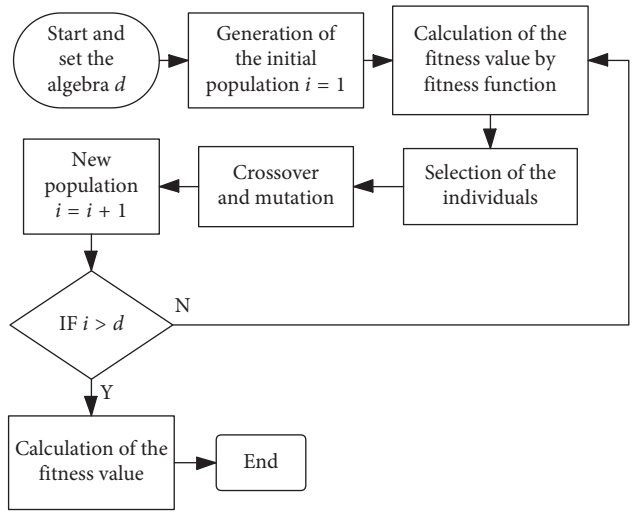

Figure 2: Flow diagram of the GA program.

3.1.2. Generation of Initial Population. The initial population is randomly picked between the stated bound of each parameter. The bound of the fifth-wheel stiffness, roll stiffness, and cornering stiffness is obtained by the output of the vehicle model simulated in the software TruckSim. The TST model in TruckSim is designed based on the parameters of the JAC-HFC4251P1K7E33ZTF6×2 tractor and Luyue LHX9406 semitrailer, which are used in the real vehicle test. The parameters of the TST are shown in Tables 3 and 4.

Table 2: Parameters of the fitness function.

Parameter	Symbol	Unit
Tractor sideslip angle of the model	$\beta_{t-\text{model}}$	Rad
Semitrailer sideslip angle of the model	$\beta_{s-\text{model}}$	Rad
Tractor yaw rate of the model	$\dot{\varphi}_{t-\text{model}}$	Rad/s
Semitrailer yaw rate of the model	$\dot{\varphi}_{s-\text{model}}$	Rad/s
Tractor roll rate of the model	$\dot{\theta}_{t-\text{model}}$	Rad/s
Semitrailer roll rate of the model	$\dot{\theta}_{s-\text{model}}$	Rad/s
Tractor roll of TruckSim	$\theta_{t-\text{model}}$	Rad
Semitrailer roll of TruckSim	$\theta_{s-\text{model}}$	Rad
Tractor sideslip angle of TruckSim	$\beta_{t-\text{trucksim}}$	Rad
Semitrailer sideslip angle of TruckSim	$\beta_{s-\text{trucksim}}$	Rad
Tractor yaw rate of TruckSim	$\dot{\varphi}_{t-\text{trucksim}}$	Rad/s
Semitrailer yaw rate of TruckSim	$\dot{\varphi}_{s-\text{trucksim}}$	Rad/s
Tractor roll rate of TruckSim	$\dot{\theta}_{t-\text{trucksim}}$	Rad/s
Semitrailer roll rate of TruckSim	$\dot{\theta}_{s-\text{trucksim}}$	Rad/s
Tractor roll of TruckSim	$\theta_{t-\text{trucksim}}$	Rad
Semitrailer roll of TruckSim	$\theta_{s-\text{trucksim}}$	Rad
Sampling point	i	—
Sampling number	b	—

Table 3: Parameters of the fully loaded JAC-HFC4251P1K7E33ZTF tractor.

Parameter	Unit	Value
Entire mass	kg	9420
Sprung mass	kg	6300
Distance between the front axle and the middle axle	m	3.37
Distance between the middle axle and the rear axle	m	1.38
Wheelbase of the front axle	m	2.04
Wheelbase of the middle and rear axles	m	1.88
Height of the CG	m	1.37
Distance between the CG and the middle axle	m	2.11
Distance between the CG and the fifth wheel	m	2.61
Distance between the CG and the roll axle line	m	1.03
Roll moment of inertia of sprung mass	kg·m^2	17260
Yaw moment of inertia of sprung mass	kg·m^2	18256
Minimum turning radius	m	16.8
Steering ratio	—	25

Table 4: Parameters of the fully loaded Luyue LHX9406 semitrailer.

Parameter	Unit	Value
Entire mass	kg	39140
Sprung mass	kg	36720
Distance between axles	m	1.31
Distance between the fifth wheel and the front axle	m	6.20
Wheelbase	m	1.84
Height of the CG	m	1.80
Distance between the CG and the front axle	m	4.65
Distance between the CG and the fifth wheel	m	3.79
Distance between the CG and the roll axle line	m	1.45
Roll moment of inertia of sprung mass	kg·m^2	21690
Yaw moment of inertia of sprung mass	kg·m^2	346782

The estimated fifth-wheel stiffness ($K_{f-\text{est}}$), roll stiffness of the tractor ($K_{rt-\text{est}}$) and semitrailer ($K_{rs-\text{est}}$), and cornering stiffness of the tractor ($K_{ct-\text{est}}$) and semitrailer ($K_{cs-\text{est}}$) are given by equation (8). By the way, the cornering stiffness of the tractor's front axle and rear axle is estimated as the same value to set the identification range:

$$\begin{cases} K_{f-\text{est}} = \dfrac{M_{\text{hitch}}}{\theta_t - \theta_s}, \\ K_{rt-\text{est}} = \dfrac{a_t m_t}{\theta_t}, \\ K_{rs-\text{est}} = \dfrac{a_s m_s}{\theta_s}, \\ K_{ct-\text{est}} = \dfrac{a_t m_t l_t}{\theta_t}, \\ K_{cs-\text{est}} = \dfrac{a_s m_s l_s}{\theta_s}, \end{cases} \tag{8}$$

where M_{hitch} is the torque on the hitch point between the tractor and the semitrailer, a_t and a_s are the lateral acceleration of the tractor and semitrailer, m_t and m_s are the sprung mass of the tractor and semitrailer, and θ_t and θ_s are the roll angle of the tractor and semitrailer.

The identification ranges of each stiffness value are set from 50% to 200% of the estimated stiffness in equation (8).

3.1.3. Selection for Evolution. According to the fitness function, the identified parameters are closer to the optimal value when the value of fitness is smaller. The individuals with a higher fitness value should be more likely to be chosen. The probability of being selected for each individual is shown as

$$\text{Prob}_p = \frac{1/f_p}{\sum_{j=0}^{p_0} 1/f_j}, \tag{9}$$

where p is the serial number of individuals, f_p is the fitness value of the p_{th} individual, and p_0 is the total number of individuals.

In the next generation, there are still p_0 individuals. Therefore, p_0 individuals are selected based on the probability calculated by equation (9) [23].

3.1.4. Crossover and Mutation. The crossover and mutation operators are used to turn the chosen individuals to new individuals in the next generation. The operators are designed by referring to the study in [24, 25].

3.2. Stiffness Identification Based on MGA. The multistage genetic algorithm is proposed to improve the precision of identification and avoid the local optimal solution problems. The fitness function, selection, crossover, and mutation in the MGA are the same as those in the GA, as shown in Section 3.1. Six key parameters are divided into two groups. The first group (fifth-wheel stiffness, roll stiffness of the tractor, and roll stiffness of the semitrailer) is identified firstly, when the second group (cornering stiffness of the

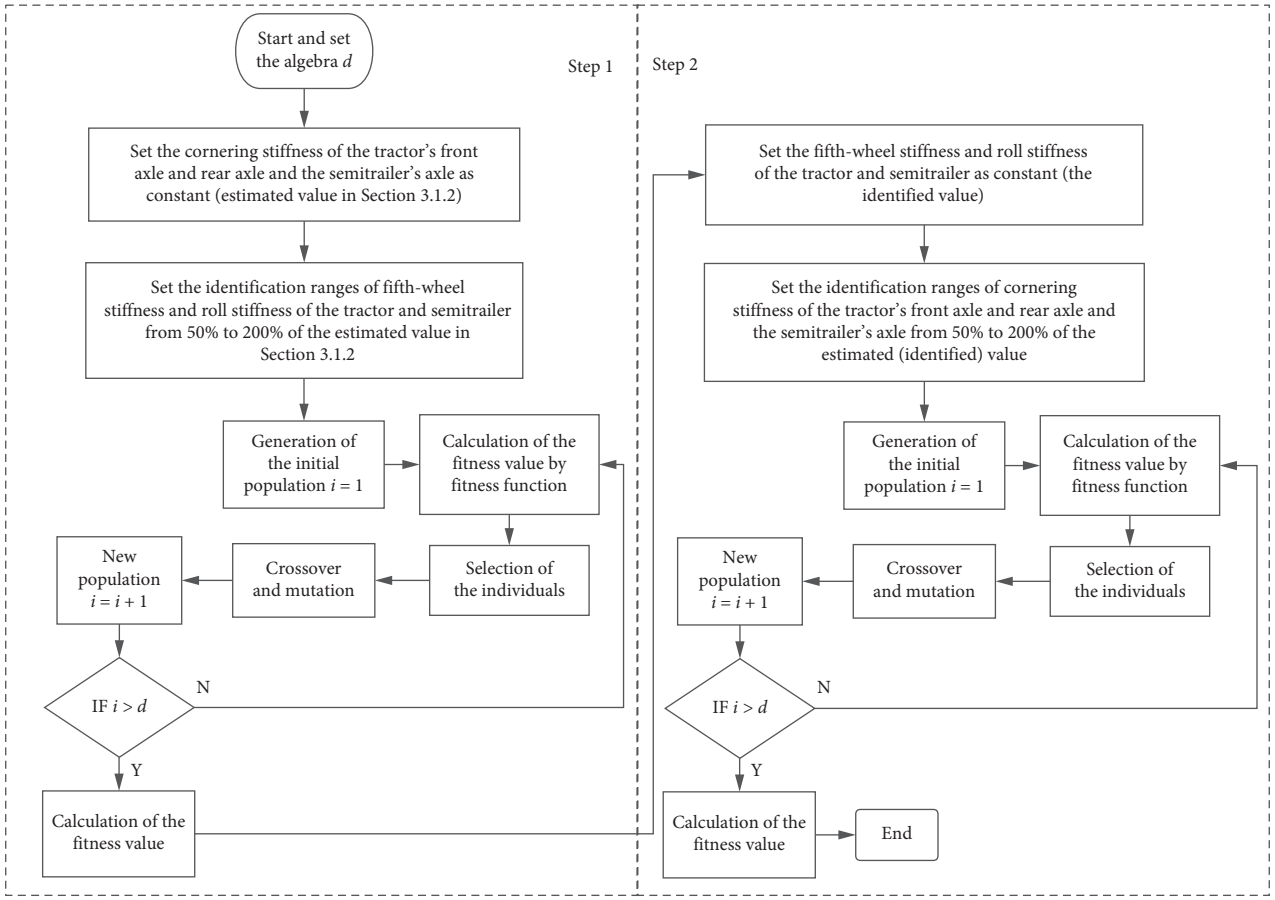

Figure 3: Flow diagram of the MGA program.

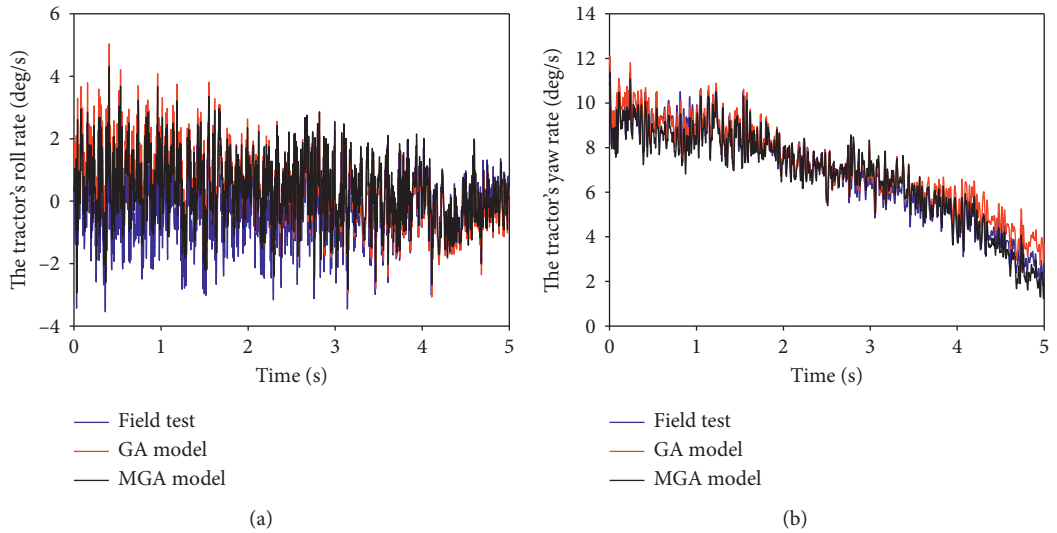

Figure 4: Output data of the field test and model based on the GA and MGA: (a) tractor's roll rate; (b) tractor's yaw rate.

tractor's front axle and rear axle and the semitrailer's axle) is set as constant, as estimated in Section 3.1.2. After identification of the first group, the identified values are set as constant, and the second group is identified, when the first group identified in the previous step is set as constant. Step 2 can be repeated until the objectives are under complete convergence. The flow diagram of the MGA program is shown in Figure 3.

The MGA can significantly improve the efficiency and precision of identification. The precision comparison between the GA and the MGA is shown in Figure 4. The output data of the model built with the parameters identified by the

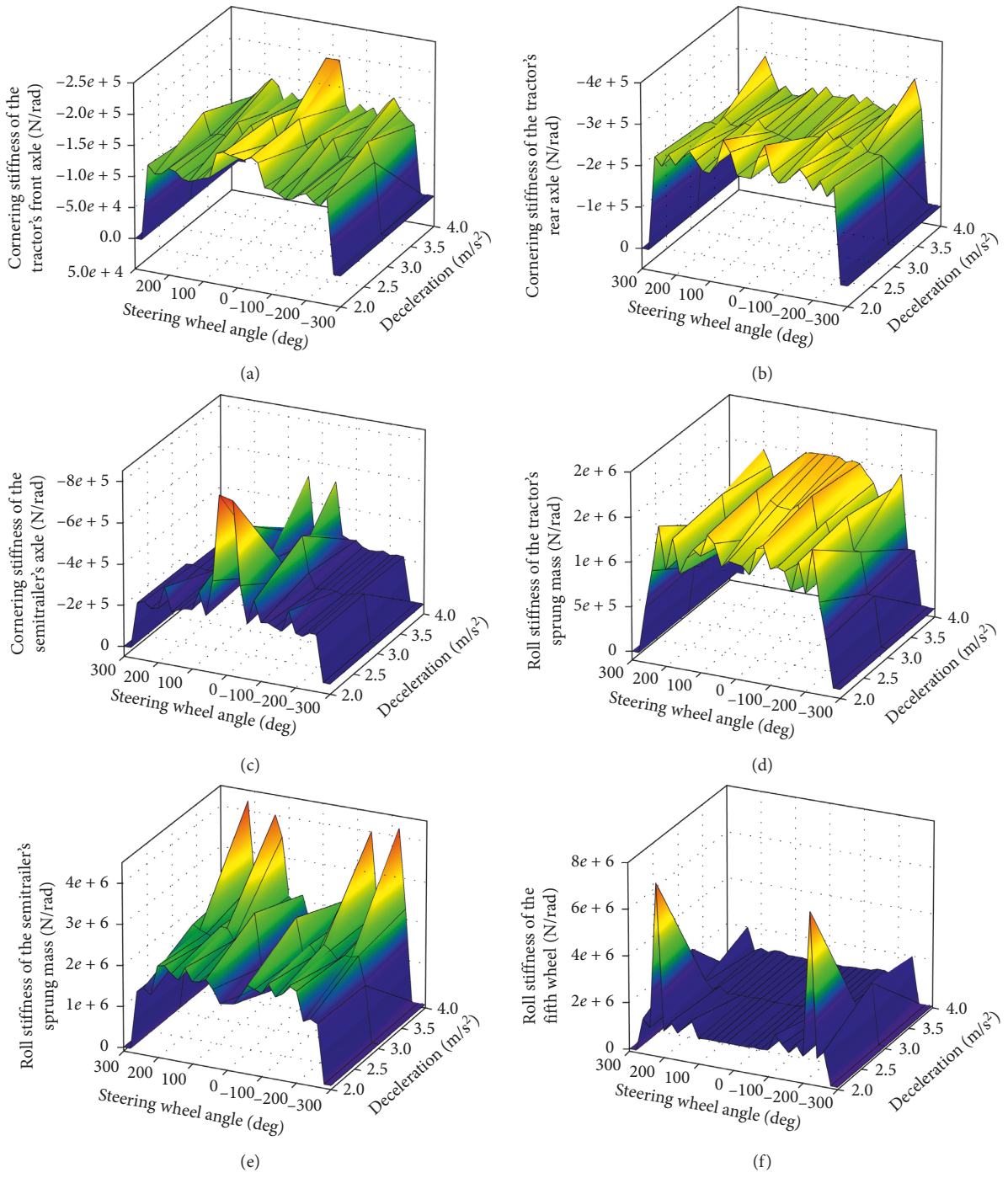

Figure 5: Key parameter maps at the initial vehicle speed of 20 km/h: (a) cornering stiffness of the tractor's front axle; (b) cornering stiffness of the tractor's rear axle; (c) cornering stiffness of the semitrailer's axle; (d) roll stiffness of the tractor's sprung mass; (e) roll stiffness of the semitrailer's sprung mass; (f) roll stiffness of the fifth wheel.

MGA are more close to the field test data than those identified by the GA. The error of the tractor's yaw rate between the field test and the model based on the GA and MGA is 10.1% and 8.0%, respectively.

3.3. Stiffness Maps. The key parameters of the linear 5-DOF model are identified offline during steering and braking at specified initial vehicle speeds, vehicle deceleration, and steering angle. The key parameters are identified by the MGA. The input data are obtained by the nonlinear simulation software TruckSim. The tractor-semitrailer model in TruckSim is designed based on the real vehicle used in the field test. The parameters of the real tractor-semitrailer are shown in Tables 3 and 4.

The typical condition for identification covers low speed to high speed, and the area of conditions covers linearity to nonlinearity. The range of the vehicle deceleration is from 2

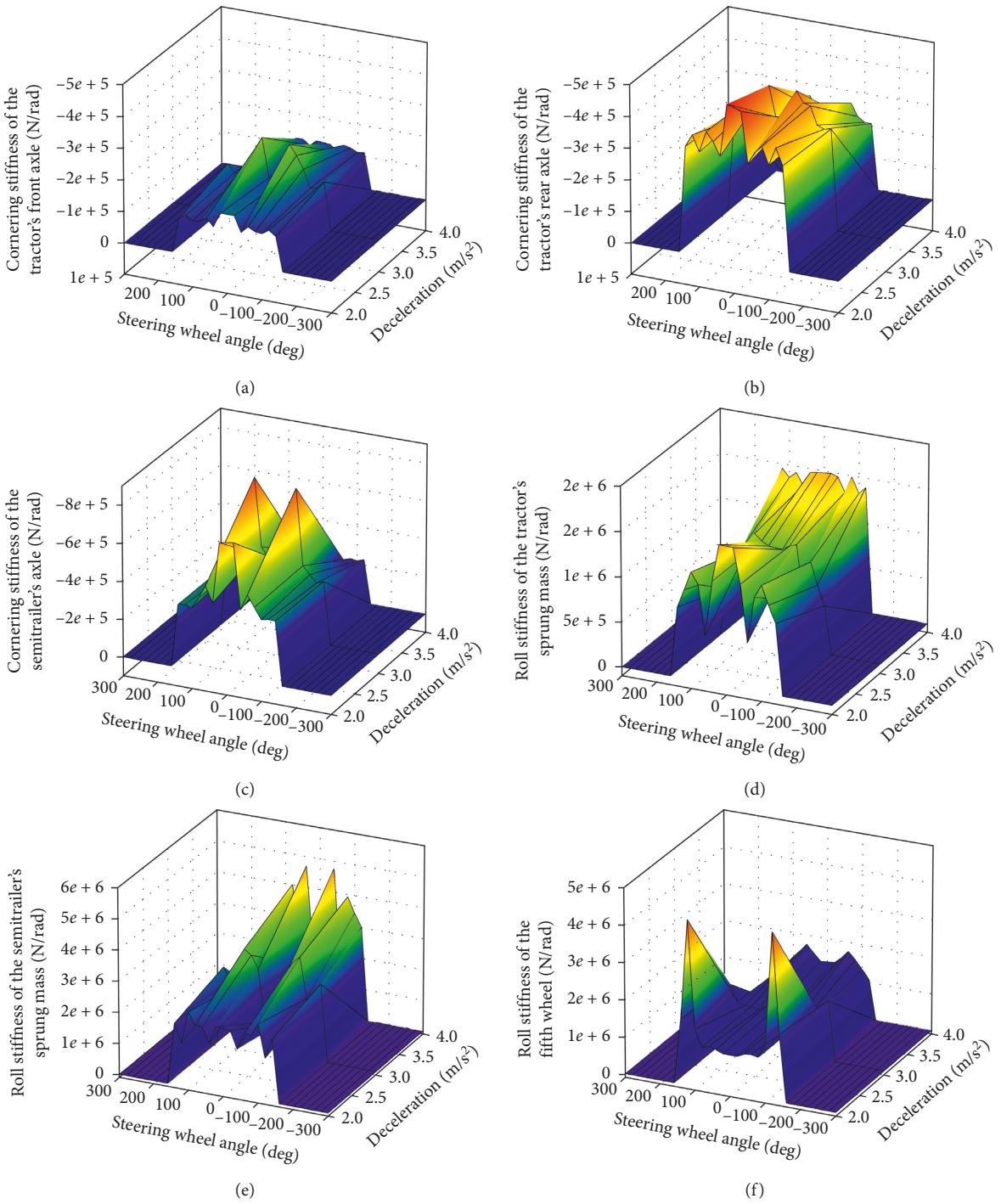

FIGURE 6: Key parameter maps at the initial vehicle speed of 60 km/h: (a) cornering stiffness of the tractor's front axle; (b) cornering stiffness of the tractor's rear axle; (c) cornering stiffness of the semitrailer's axle; (d) roll stiffness of the tractor's sprung mass; (e) roll stiffness of the semitrailer's sprung mass; (f) roll stiffness of the fifth wheel.

to 4 m/s^2, and the range of steering wheel angle is from −300 to 300°. The initial vehicle speed is 20 and 60 km/h [26, 27]. The interval of operating points is set by the deceleration of 1 m/s^2 and the steering wheel angle of 20°. When the vehicle is in rollover, the parameter values of maps are set to zero. When the parameter identification of designed points is completed, the maps of key parameters are formed by the software SigmaPlot using the identified parameter values. To ensure that the key parameters of the model can change with the variation of the real-time vehicle states, the key parameter values under any initial vehicle speed, deceleration, and steering wheel angle can easily be obtained by using piecewise linear interpolation according to the maps. The maps of the identified key parameters are shown in Figures 5 and 6.

Figure 7: Experimental tractor and semitrailer.

(a) (b) (c) (d) (e) (f)

Figure 8: Data acquisition equipment: (a) data acquisition unit; (b, c) AHRSs equipped on the tractor and semitrailer; (d) steering wheel sensor; (e) brake pedal sensor; (f) road friction coefficient sensor.

4. Field Tests during Steering and Braking

To verify the reliability of the 5-DOF model with identified parameter maps, an experimental TST was used in accordance with the reference vehicle in building the TruckSim model, as shown in Figure 7. It consists of a JAC-HFC4251P1K7E33ZTF6×2 tractor, pulling a Luyue LHX9406 semitrailer. The trailer was loaded with dry sand. The Naiou-KD-10 GPS was equipped on the top of the tractor. Two Xsens MTi-30 attitude and heading reference systems (AHRSs) were, respectively, equipped, as shown in Figures 8(b) and 8(c). The ZC-2A angle sensor of the steering

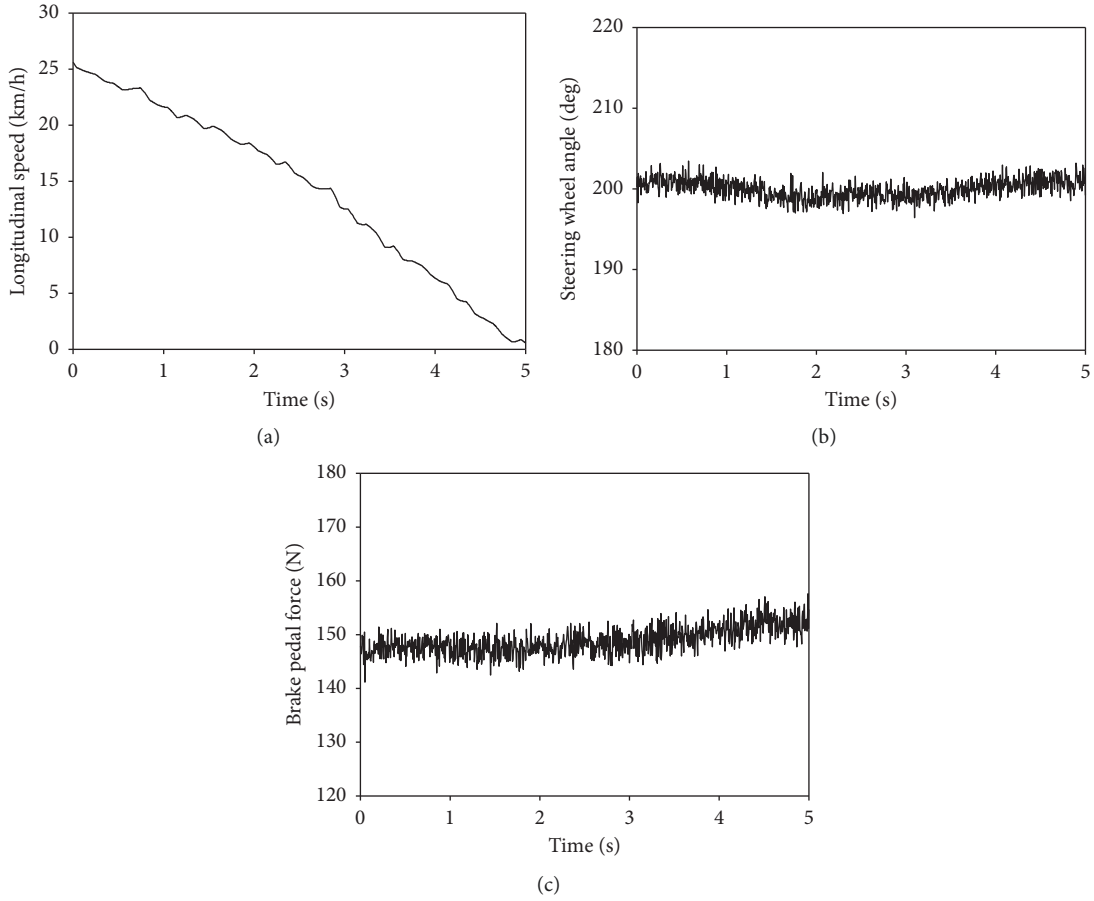

Figure 9: Steering and braking field test: (a) longitudinal speed; (b) steering wheel angle; (c) brake pedal force.

wheel and JYT-B brake pedal force sensor were equipped in the cab, as shown in Figures 8(d) and 8(e).

The test was carried out in the performance testing ground of Dingyuan Proving Ground for Vehicle, General Administration of Quality Supervision, Inspection and Quarantine of the P.R.C. The steering and braking experiment is designed based on the Chinese national standards GB/T 13594-2003 and GB 12676-2014. The testing ground is a flat cement area. The road friction coefficient is 0.62, measured by the Yisai-JN-1 road friction coefficient sensor in Figure 8(f). Before the test, the vehicle had run 10 minutes at 30 km/h to make the vehicle warm up gradually. Then, the vehicle ran around the curve at 25 km/h and broke in 5 seconds. The brake pedal force and steering wheel angle were stabilized, as shown in Figures 9(b) and 9(c). The data shown in Table 5 were collected. Vibrations due to road roughness, the engine, and aerodynamics can cause some unwanted noises. So the original data are filtered by the Filter Design and Analysis Tool in the software MATLAB. The longitudinal speed of the tractor is shown in Figure 9(a). When the vehicle speed is lower than 5 km/h, the vehicle body is strongly unstable. So the test data from 0 to 5 km/h were ignored in analysis.

Table 5: Attitude parameters of the TST.

Attitude parameters	Unit
Tractor speed	km/h
Steering wheel angle	Rad
Brake pedal force	N
Tractor yaw rate	Rad/s
Semitrailer yaw rate	Rad/s
Tractor roll angle	Rad
Semitrailer roll angle	Rad
Tractor roll rate	Rad/s
Semitrailer roll rate	Rad/s

5. Data Processing and Verification

The original outputs of the field test were filtered by the Hamming window filter based on the Filter Design and Analysis Tool in MATLAB. The yaw rate, roll rate, and roll angle of the TST of the 5-DOF model with parameter maps were contrasted with the field test data.

The typical outputs of the TST state variables of the 5-DOF model and test vehicle are shown in Figure 8. In Figures 10(a) and 10(b), it can be seen that the roll angle of

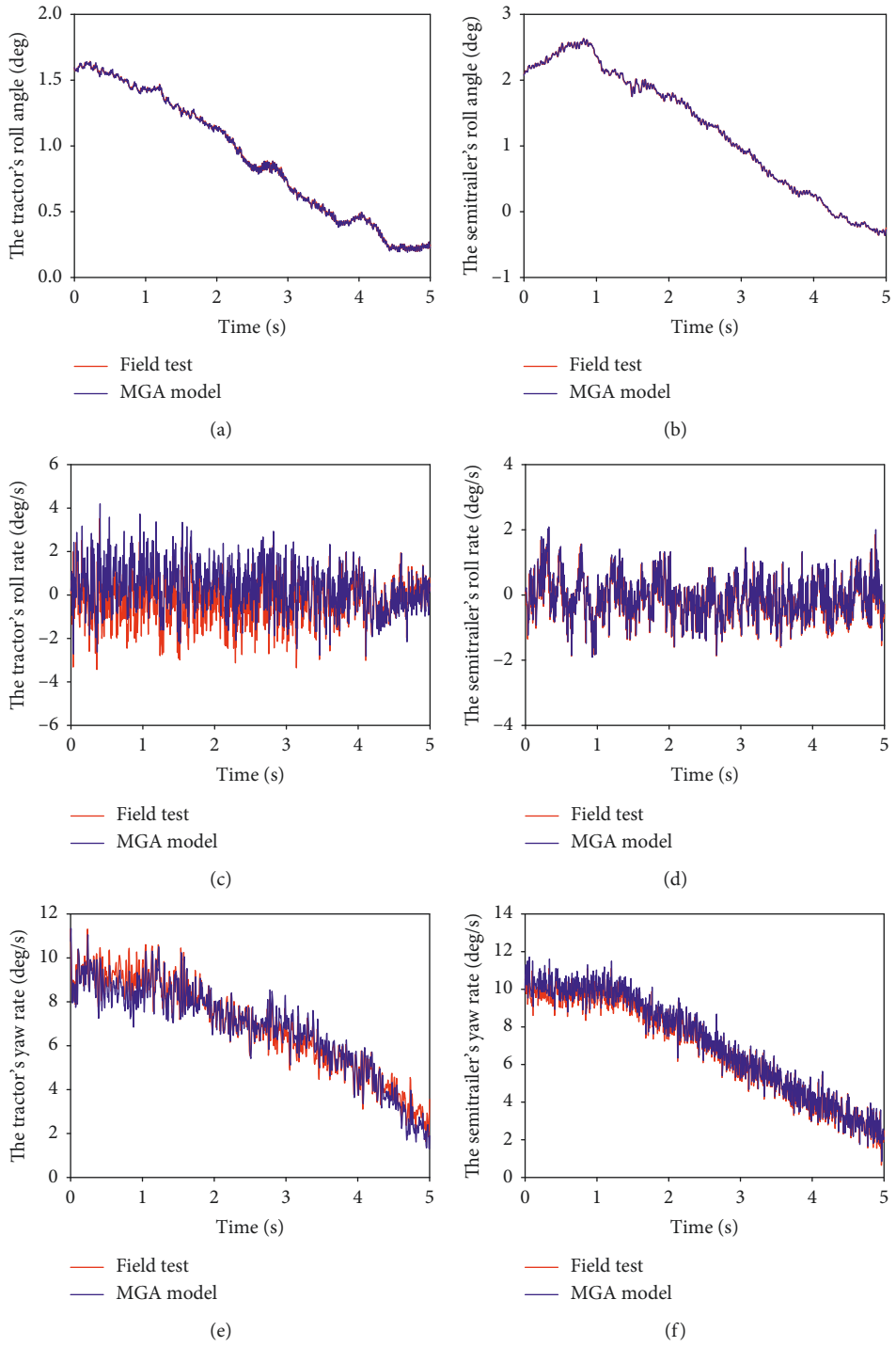

Figure 10: 5-DOF model data and field test data: (a) tractor's roll angle; (b) semitrailer's roll angle; (c) tractor's roll rate; (d) semitrailer's roll rate; (e) tractor's yaw rate; (f) semitrailer's yaw rate.

the 5-DOF model are similar to that of the field test. The average errors of the tractor's roll angle and semitrailer's roll angle are 1.13% and 1.24%, respectively. In Figures 10(c)–10(f), the roll rate and yaw rate are in good agreement. The average errors of the tractor and semitrailer's yaw rate between the model and the test vehicle are 8.0% and 11.3%, respectively. In the equations of vehicle motions, the roll angles are of the first order. The roll rate and yaw rate are the derivative terms which are harder to calculate. As a result, the errors of the roll rate and yaw rate are much higher than that of the roll angle.

6. Conclusion

This paper focused on the accurate linear TST model. The following conclusions can be drawn from this study:

(1) The 5-DOF linear TST model has been presented. The roll stiffness, axle cornering stiffness, and fifth-wheel stiffness were assumed to be constant at any specified initial longitudinal speeds, longitudinal deceleration, and steering angle.

(2) The longitudinal deceleration and steering wheel angle were set as the input variable to figure out their relationships with identification parameters.

(3) The GA and MGA were applied to identify the key parameters of the 5-DOF model. The MGA was proved to be more precise than the GA. The objective function (fitness function) is the absolute value of error between the outputs of the simplified 5-DOF tractor-semitrailer model and TruckSim. The key parameter maps were formed at the initial speed of 20 km/h and 60 km/h.

(4) The identification results show that the fifth-wheel stiffness is not absolutely constant when the longitudinal deceleration and steering wheel angle change. The fifth-wheel stiffness is stable when the steering wheel angle is small. But when the steering wheel angle is close to the extreme area, the fifth-wheel stiffness is increased dramatically.

(5) Running with online interpolation of the key parameters based on the offline maps, the 5-DOF model output is compared with the field test data. The results showed that model outputs of the simplified model and real vehicle agree well.

Appendix

The nonzero elements of M and A

The nonzero elements of **M** and **A** are as follows:

$$
\begin{aligned}
M_{11} &= m_t v_{tx} l_3,\\
M_{21} &= m_t v_{tx} h_{tF} - M_t v_{tx} h_t,\\
M_{51} &= l_3,\\
M_{61} &= m_t v_{tx},\\
M_{12} &= I_{tzz},\\
M_{13} &= -m_t h_t l_3,\\
M_{23} &= I_{txx} + M_t h_t^2 - m_t h_t h_{tF},\\
M_{63} &= -m_t h_t,\\
M_{74} &= 1,\\
M_{35} &= -m_s v_{sx} l_4,\\
M_{45} &= m_s v_{sx} h_{sF} - M_s v_{sx} h_s,\\
M_{55} &= l_4,\\
M_{65} &= m_s v_{sx},\\
M_{36} &= I_{szz},\\
M_{37} &= m_s h_s l_4,\\
M_{47} &= I_{sxx} + M_s h_s^2 - m_s h_s h_{sF},\\
M_{67} &= -m_s h_s,\\
M_{88} &= 1,\\
A_{11} &= K_1 (l_1 + l_3) + K_2 (l_3 - l_2),\\
A_{21} &= (K_1 + K_2) h_{tF},\\
A_{61} &= K_1 + K_2,\\
A_{12} &= \frac{\left(K_1 l_1^2 + K_2 l_2 l_3 + K_1 l_1 l_3 - K_3 l_3^2\right)}{v_{tx}} - m_t v_{tx} l_3,\\
A_{22} &= (M_t h_t - m_t h_{tF}) v_{tx} + \frac{(K_1 l_1 - K_2 l_3) h_{tF}}{v_{tx}},\\
A_{52} &= -l_3,\\
A_{62} &= -m_t v_{tx} + \frac{(K_1 l_1 - K_2 l_3)}{v_{tx}},\\
A_{23} &= -C_{rt},\\
A_{53} &= -h_{tF},\\
A_{73} &= 1,\\
A_{24} &= m_t g h_t - K_{rt} - K_F,\\
A_{44} &= K_F,\\
A_{35} &= -K_3 (l_4 + l_5),\\
A_{45} &= K_3 h_{sF},\\
A_{65} &= K_3,\\
A_{36} &= \frac{K_3 (l_4 + l_5) l_5}{v_{sx}} + m_s v_{sx} l_4,\\
A_{46} &= M_s v_{sx} h_s - m_s v_{sx} h_{sF} - \frac{K_3 l_5 h_{sF}}{v_{sx}},\\
A_{56} &= -l_4,\\
A_{66} &= -m_s v_{sx} - \frac{K_3 l_5}{v_{sx}},\\
A_{47} &= -C_{rs},\\
A_{57} &= h_{sF},\\
A_{87} &= 1,\\
A_{28} &= K_F,\\
A_{48} &= m_s g h_s - K_{rs} - K_F.
\end{aligned}
\tag{A.1}
$$

Data Availability

The data used to support the findings of this study are available from the corresponding author upon request.

Conflicts of Interest

The authors declare that they have no conflicts of interest.

Acknowledgments

The authors would like to thank the School of Automotive and Transportation Engineering, Hefei University of Technology, Hefei, Anhui, P.R.C., as well as the National Natural Science Foundation of China (Grant No. 71431003), the Research Project of University Natural Science of Anhui Province (Grant No. KJ2018A0782), and the General Research Project of Anhui University Management Big Data Research Center (Grant No. 2016015).

References

[1] B. A. Jujnovich and D. Cebon, "Path-following steering control for articulated vehicles," *Journal of Dynamic Systems, Measurement, and Control*, vol. 135, no. 3, Article ID 031006, 2013.

[2] M. M. Islam and Y. He, "A parallel design optimisation method for articulated heavy vehicles with active safety systems," *International Journal of Heavy Vehicle Systems*, vol. 20, no. 4, p. 327, 2013.

[3] Y. Nakamura, H. Ezaki, Y. Tan, and W. Chung, "Design of steering mechanism and control of nonholonomic trailer systems," *IEEE Transactions on Robotics and Automation*, vol. 17, no. 3, pp. 367–374, 2001.

[4] J. Wideberg and E. Dahlberg, "Effect of the fifth-wheel placement on the stability of articulated vehicles," *International Journal of Heavy Vehicle Systems*, vol. 20, no. 2, p. 144, 2013.

[5] L. Segel, "Research in the fundamentals of automobile control and stability," in *Proceedings of the SAE Technical Paper Series*, vol. 1, 1957.

[6] Q. Wang and Y. He, "A study on single lane-change manoeuvres for determining rearward amplification of multi-trailer articulated heavy vehicles with active trailer steering systems," *Vehicle System Dynamics*, vol. 54, no. 1, pp. 102–123, 2016.

[7] X. Ding, S. Mikaric, and Y. He, "Design of an active trailer-steering system for multi-trailer articulated heavy vehicles using real-time simulations," *Proceedings of the Institution of Mechanical Engineers, Part D: Journal of Automobile Engineering*, vol. 227, no. 5, pp. 643–655, 2013.

[8] S. Kharrazi, M. Lidberg, and J. Fredriksson, "A generic controller for improving lateral performance of heavy vehicle combinations," *Proceedings of the Institution of Mechanical Engineers, Part D: Journal of Automobile Engineering*, vol. 227, no. 5, pp. 619–642, 2013.

[9] S. H. Tabatabaei Oreh, R. Kazemi, and S. Azadi, "A sliding-mode controller for directional control of articulated heavy vehicles," *Proceedings of the Institution of Mechanical Engineers, Part D: Journal of Automobile Engineering*, vol. 228, no. 3, pp. 245–262, 2014.

[10] S. H. T. Oreh, R. Kazemi, and S. Azadi, "A new method for off-tracking eliminating in a tractor semi-trailer," *International Journal of Heavy Vehicle Systems*, vol. 23, no. 2, p. 107, 2016.

[11] H. Yu, L. Güvenc, and Ü. Özgüner, "Heavy-duty vehicle rollover detection and active roll control," *IFAC Proceedings Volumes*, vol. 38, no. 1, pp. 128–133, 2005.

[12] F. Saglam and Y. S. Unlusoy, "Identification of low order vehicle handling models from multibody vehicle dynamics models," in *Proceedings of the 2011 IEEE International Conference on Mechatronics, ICM 2011*, pp. 96–101, Istanbul, Turkey, April 2011.

[13] Z. G. Nie and C. F. Zong, "A study on the parameters identification of simplified models for articulated heavy vehicles," *Automotive Engineering*, vol. 37, no. 6, pp. 622–630, 2015.

[14] Z. G. Nie and C. F. Zong, "Parameters identification for simplified yaw model of articulated heavy vehicle," *Advanced Materials Research*, vol. 765-767, pp. 387–391, 2013.

[15] K.-I. Kim, H. Guan, B. Wang, R. Guo, and F. Liang, "Active steering control strategy for articulated vehicles," *Frontiers of Information Technology & Electronic Engineering*, vol. 17, no. 6, pp. 576–586, 2016.

[16] H. Guan, K. Kim, and B. Wang, "Comprehensive path and attitude control of articulated vehicles for varying vehicle conditions," *International Journal of Heavy Vehicle Systems*, vol. 24, no. 1, p. 65, 2017.

[17] H. Dahmani, M. Chadli, A. Rabhi, and A. El Hajjaji, "Vehicle dynamic estimation with road bank angle consideration for rollover detection: theoretical and experimental studies," *Vehicle System Dynamics*, vol. 51, no. 12, pp. 1853–1871, 2013.

[18] J. H. Holland, *Adaptation in Natural and Artificial Systems*, MIT Press, Cambridge, MA, USA, 1992.

[19] E. Ursu and J.-C. Pereau, "Robust modelling of periodic vector autoregressive time series," *Journal of Statistical Planning and Inference*, vol. 155, pp. 93–106, 2014.

[20] M. M. Islam, Y. He, S. Zhu, and Q. Wang, "A comparative study of multi-trailer articulated heavy-vehicle models," *Proceedings of the Institution of Mechanical Engineers, Part D: Journal of Automobile Engineering*, vol. 229, no. 9, pp. 1200–1228, 2015.

[21] P. Fancher and C. Winkler, "Directional performance issues in evaluation and design of articulated heavy vehicles," *Vehicle System Dynamics*, vol. 45, no. 7-8, pp. 607–647, 2007.

[22] G. Baffet, A. Charara, and D. Lechner, "Estimation of vehicle sideslip, tire force and wheel cornering stiffness," *Control Engineering Practice*, vol. 17, no. 11, pp. 1255–1264, 2009.

[23] M. Morini and S. Pellegrino, "Personal income tax reforms: a genetic algorithm approach," *European Journal of Operational Research*, vol. 264, no. 3, pp. 994–1004, 2018.

[24] J. A. Cabrera, A. Ortiz, E. Carabias, and A. Simon, "An alternative method to determine the magic tyre model parameters using genetic algorithms," *Vehicle System Dynamics*, vol. 41, no. 2, pp. 109–127, 2004.

[25] M. Sergeeva, D. Delahaye, C. Mancel, and A. Vidosavljevic, "Dynamic airspace configuration by genetic algorithm," *Journal of Traffic and Transportation Engineering (English Edition)*, vol. 4, no. 3, pp. 300–314, 2017.

[26] I. and Q. of P. R. C. & S. A. of P. R. C. General Administration of Quality Supervision, *Technical Repuirements and Testing Methods for Commercial Vehicle and Trailer Braking Systems*, General Administration of Quality Supervision, Beijing, China, 2014.

[27] I. and Q. of P. R. C. General Administration of Quality Supervision, *Antilock Braking Performance and Test Procedure for Motor Vehicles and Their Trailers*, General Administration of Quality Supervision, Beijing, China, 2003.